



Advanced magnetic resonance techniques in early differentiation of pseudoprogression versus progression in the patients with glioblastoma multiforme

Napredne tehnike magnetne rezonance u ranom razdvajanju pseudoprogresije od progresije kod bolesnika sa glioblastomom multiforme

Jelena Mihailović*, Marko Daković†

Institute for Oncology and Radiology of Serbia, *Department for Diagnostic Radiology, Belgrade, Serbia; University of Belgrade, †Faculty for Physical Chemistry, Belgrade, Serbia

Abstract

Background/Aim. The diagnosis of glioblastoma multiforme progression may be confounded by a phenomena termed pseudoprogression (PSP) and pseudoresponse (RCT) which has become more common with the adoption of radiation therapy with concurrent and adjuvant application of temozolomide (CRT). Distinguishing of these phenomena is based on the follow-up scans since no single imaging method or technique is yet capable of performing their discrimination. In this study, we evaluated the dynamic susceptibility contrast (DSC perfusion) imaging and magnetic resonance (MR) spectroscopy to predict the prognosis and time to progression in the patients with glioblastoma multiforme. **Methods.** Forty patients with primary glioblastoma multiforme were included in the analysis. The patients were examined in 3rd week after surgery and 10th week after the beginning of CRT. The MR exams were performed using the 1.5 T MR scanner (Avanto; Siemens, Erlangen, Germany). The maps of perfusion parameters and time-to-peak (TTP) parameter were calculated using the DPTools v3.79 software. The 3D CSI PRESS MR spectroscopy was performed in the area corresponding to the con-

trast enhancement on the T1W images. **Results.** Thirty-two of the 40 patients had progressive disease and 8 had pseudoprogression. Progressive disease showed the mean time of the peak values of 33 ± 7 s in 3rd and 30 ± 5 s in 10th week with no statistical significance between these two periods ($p > 0.05$). The patients with pseudoprogression showed the mean time of the peak values of 32 ± 8 s in 3rd week and 43 ± 9 s in 10th week; it was statistically significant difference ($p < 0.05$) which favors better response to therapy. The spectroscopy results showed presence of glycine peak at 3.56 ppm in 6 patients with progressive disease which was not seen on spectra with pseudoprogression. **Conclusion.** The observed significant differences in the TTP values for PSP and RCT can provide basis for distinguishing two entities. The presence of glycine peak in the MR spectra could be a marker of RCT.

Key words:

glioblastoma; disease progression; drug therapy; radiotherapy; surgical procedures, operative; magnetic resonance imaging; spectrum analysis; diagnosis, differential.

Apstrakt

Uvod/Cilj. Uvođenje tretmana glioblastoma zračnom terapijom uz konkurentnu i adjuvantnu primenu temozolomida (CRT) dovelo je do pojave nove dijagnostičke dileme – potrebe za razlikovanjem pseudo-progresije i presudoodgovora. Razlikovanje snimaka magnetne rezonance (MR) ova dva fenomena za sada je moguće samo evaluacijom u više vremenskih tačaka u toku terapije, dok nove tehnike koje bi pomogle u njihovom razlikovanju nisu još uvedene. U radu je analizirana mogućnost primene *time-to-peak* (TTP) mapa dinamičkog perfuzionog imidžinga i magnetno rezonantne spektroskopije u utvrđivanju odgovora tumora na terapiju.

Metode. Analizirano je 40 bolesnika sa primarnim glioblastomom multiforme. Bolesnici su snimani u trećoj nedelji nakon operacije i desetoj nedelji od početka CRT. Pregledi na aparatu za MR rađeni su na aparatu 1.5 T Avanto Siemens, Erlangen Nemačka. Mape perfuzionih parametara generisane su i analizirane korišćenjem programa DPtools v3.79. 3D CSI PRESS spektroskopija sa dugim i kratkim vremenom eha rađena je kod svih bolesnika. **Rezultati.** Kod 32 od 40 bolesnika dijagnostikovana je progresija bolesti, a kod osam je dijagnostikovana pseudo-progresija. Kod bolesnika sa progresijom bolesti dobijene *time-to-peak* vrednosti su bile 33 ± 7 s u trećoj nedelji i 30 ± 5 s u desetoj nedelji, što ne predstavlja statistički značajnu razliku. Vredno-

sti ovog parametra za pseudoprogresiju bile su 32 ± 8 s u trećoj i 43 ± 9 s u desetoj nedelji što je statistički značajna razlika ($p < 0.05$). Rezultati spektroskopije ukazali su na prisustvo glicinskog pika kod šest bolesnika sa progresijom bolesti, dok kod pseudoprogresije ovaj metabolit nije bio prisutan. **Zaključak.** Analizirani MR snimci pokazali su da je MR veoma uspešna tehniku za postavljanje dijagnoze pro-

gresije bolesti tokom terapije kod bolesnika sa glioblastomom.

Ključne reči:

glioblastom; bolest, progresija; lečenje lekovima; radioterapija; hirurgija, operativne procedure; magnetna rezonanca, snimanje; spektar, analize; dijagnoza, diferencijalna.

Introduction

Glioblastoma multiforme (GBM) is the most common brain tumor characterized by high aggressiveness and poor outcome. The current standard of treatment is surgical resection, followed by concomitant chemotherapy (CM) and radiotherapy (RT) ^{1, 2}. The evaluation of GBM response to therapy is guided by several criteria which consider findings in the post-treatment radiological and clinical evaluation. According to Macdonald et al. ³, the tumor recurrence (RCT) can be established by presence of 25% increase in the post-contrast T1W magnetic resonance images (MRI) and clinical deterioration. Recently adopted RANO (Response Assessment in Neuro-Oncology) ⁴ criterion states that, within period of 12 weeks upon completion of RT, a true progression can only be established if a majority of new post-contrast enhancement in the T1W images appears in region outside the area treated by the RT. However, the introduction of the new first-line chemotherapeutic temozolomide (TMZ) led to observation of a relatively new phenomenon in the follow-up of GBM treatment – pseudoprogresion (PSP). PSP is a phenomenon of subacute changes observed in the glioma imaging, subsequent to radiochemotherapy, suggestive of progression, with or without associated clinical sequelae, which resolve spontaneously without further therapy ⁵. In contrast to radiation necrosis which appears months to several years after RT ⁶, PSP usually can be observed several weeks after RT ⁷. Beside the similar appearance of PSP and RCT on the post-contrast T1W images, the first could be also followed by clinical deterioration. The correct distinguishing of PSP and RCT has a large impact on decision whether TMZ application should be continued or ceased and changed with an agent specific for recurrent tumor (e.g., Avastin, etc.).

The advanced MRI methods, such as diffusion weighted imaging (DWI), perfusion imaging and magnetic resonance spectroscopy (MRS) showed variable success in distinguishing two entities. The principal obstacle in the evaluation of GBM response to therapy using DWI lies in inherently high heterogeneity of tumors appearance on the DWI and maps of the apparent diffusion coefficient (ADC), a feature which is often further increased by treatment. Chu et al. ⁸ reported that DWI obtained at the very high b -values ($3000 \text{ s}\cdot\text{mm}^{-2}$), hardly obtainable in clinical MRI setups, can be used in distinguishing PS and RCT.

Since neoangiogenesis and increased vascular density are prominent features of recurrent tumors, the techniques which enable their tracing have a large potential in differentiation of RCT from radiation necrosis. So far, there is a single report dealing with the use of dynamic contrast enhanced

(DCE) imaging in distinguishing RCT from PSP. Suh et al. ⁹ used ratios of areas under initial and, somewhat arbitrarily, selected final part of DCE curve to successfully distinguish these entities.

The perfusion parameters derived from the dynamic susceptibility weighted imaging (DSC) such as relative cerebral blood flow (rCBF), mean transition time (MTT) and particularly relative cerebral blood volume (rCBV) have been successfully used to distinguish residual/recurrent neoplasm from treatment-related radiation necrosis ^{10, 11}. Few studies reported the use of the DSC parameters in differentiation of RCT and PSP, although with variable success. Song et al. ¹² reported that mean rCBV cannot be used for differentiation of RCT and PSP. Kong et al. ¹³ reported that PSP showed significantly lower rCBV values compared with RCT, so they could be distinguished with cut-off value 1.45 (81.5 % sensitivity, 77.8 % specificity). There are reports that PSP and RCT can be distinguished with somewhat higher sensitivity and specificity when cut-off value 1.8 for rCBV is used ^{5, 14}. Mangla et al. ¹⁵ evaluated the rCBV values in the patients with GBM before and 1 month after RT-TMZ treatment and observed 41% decrease in rCBV in the PSP patients, in contrast to 12% increase in rCBV for the RCT patients. However, the studies dealing with classical analysis of perfusion maps suffer from several limitations. First, different modalities were used for correction of contrast leakage which is usually achieved by use of the pre-bolus application of small dose of a contrast agent or by use of a software; in some studies this correction was not used at all ¹⁴. Second, the regions of observed the increase of rCBV values may contain tissue which responded to treatment as well as viable tumor in different fractions – even a minute presence of GBM (abundant less than 5 % in total) is considered as RCT ¹⁶. There are several studies involving detailed analysis of the rCBV maps in tumor region. Baek et al. ¹⁷ used the histogram analysis of perfusion maps in two time points after completion of RT and CM and found that percentage change in the histogram parameters can be used for distinguishing PSP and RCT. Cha et al. ¹⁸ implemented complex approach by combining the histograms of ADC and rCBV maps and traced changes in their parameters between two follow-up time points. They found that difference histograms with high sensitivity and accuracy can be used for distinguishing RCT and PSP. Tsien et al. ¹⁹ used the voxel-based analysis of rCBV maps before and after received therapy and significantly lower values of this parameter in PSP when compared to the RCT patients. Hu et al. ¹⁶ used interesting approach for differentiation of PSP and RCT as well as for obtaining tumor burden in enhancing lesion. In their study a

combination of histological analysis of tumor tissue and evaluation of perfusion maps was used in obtaining the rCBV cut-off values which resulted in complete differentiation of PSP from RCT.

The time-to-peak (TTP) parameter can be determined by measuring the interval from the contrast agent administration to appearance of minimum in time course of DSC signal change. The maps of this parameter are usually generated automatically using the standard software packages built in the MRI console. However, due to a variation between the time of contrast injection and the arrival of the bolus in the cerebral arteries the comparison of absolute TTP values is difficult to compare. Therefore, in order to enable comparisons between TTP for different individuals or the examinations, the standardized TTP maps should be used²⁰. This parameter was extensively used in computed tomography (CT) for differentiation of pathologies outside the central nervous system (CNS) and in characterization of strokes, and in differentiation of GBM from solitary metastasis. However, to our knowledge, TTP derived from the DSC images has been used only for the evaluation of the stroke-affected tissue²¹, but not for the assessment of tumor response to therapy.

MRS is frequently applied as a tool for differentiation various brain pathologies. However, the discrimination power of MRS in follow-up of tumor response to therapy is limited by considerable overlapping of spectroscopic profiles of RCT and radiation/chemo therapy. This is particularly pronounced in differentiation of RCT and TMZ/RT treatment-induced PSP since both could have the same spectroscopic features including reduction of N-acetyl aspartate (NAA), elevation of choline (Cho) and a large increase in lactate/lipid concentrations^{22, 23}.

Several studies showed that the GBM cells release excitotoxic levels of glutamate in extracellular space^{24, 25}. This may lead to the increased levels of this excitatory neurotransmitter which is followed by elevation of levels of inhibitory transmitters particularly glycine (Gly). Although there is a number of biochemical studies which dealt with transport and accumulation of glycine in the GBM cells, the reasons for this remain unclear²⁶. Increased levels of Gly were also observed in some metabolic diseases, medulloblastoma and in the low grade tumor central neurocytoma.

In this study we evaluated a possibility of TTP application, as minimally subjective parameter, in distinguishing of PSP from RCT. Sensitivity and specificity of differentiation were compared to that of the routinely reported DSC parameter rCBV. The level of glycine, obtained from the analysis of MRI spectra of tumor tissue was tested as a marker for establishing presence of PSP.

Methods

Patients

This study included 40 patients with primary GBM, confirmed by histopathological analysis, (27 males and 13 females, mean age 51 years) who underwent a surgical resection followed by concomitant TMZ and RT. The treatment

protocol included RT plus continuous daily TMZ (75 mg/m²/day) followed by 6 cycles of adjuvant TMZ (150 mg/m² for 5 days every 28 days). The treatment started one week after the surgery.

Magnetic resonance imaging examination

All MRI examinations were performed using the 1.5T MR scanner (Avanto; Siemens, Erlangen, Germany) in the 3rd and 10th week upon the surgery (2nd and 9th week after starting the CMT+RT therapy). The first part of protocol included the T1W (TR/TE 550/9.4 ms), T2W (TR/TE 3808/89ms) and FLAIR imaging (TR/TE/TI 9900/126/2500). The MR examinations were repeated in the 6th month after the surgery in order to establish definitive diagnosis of PSP and RCT: a decrease of postcontrast enhancement on the T1w images was indicative to presence of PSP, otherwise RCT was diagnosed. The obtained images were reviewed by a neuroradiologist with 18 years of experience.

Dynamic susceptibility contrast

The DSC MRI was performed using a dynamic T2*-weighted echo-planar MR sequence. The multisection image data were acquired for a total of 90 s, with the bolus contrast injection occurring after 13 seconds to get a sufficient number of baseline images. The images were acquired in the axial plane with the mid-slice position at the level of the basal ganglia. A contrast medium bolus (dose, 0.1 mmol/kg Gadovist, Bayer Schering Pharma, Berlin, Germany) was administered using an MRI injector (Ulrich Medical; Mississippi™ (MRI), Germany) with a 5 mL/s flow rate.

The data from the DSC MRI were transferred to a PC workstation and analyzed using the software package DPTools (Version 3.79). Time courses of the DSC signal were obtained from four ROIs (20–30 pixels in size) placed in regions of the row DSC images corresponding to contrast enhancement in the T1W images. Arterial input function was selected by placing single ROI over the middle cerebral artery located in the hemisphere contralateral to lesion. After obtaining the rCBV maps, four ROIs (20–30 pixels) were placed within regions of the map which correspond to the contrast enhancement in the T1W images or perifocally to surgical cavity if no post-contrast enhancement was observed. rCBV associated with each positioned ROI was obtained and normalized (nCBV) by division by rCBV obtained for contralateral white matter. The DSC curves were obtained from ROIs identically positioned as previously described and averaged. The TTP parameter was determined as a time period from the application of contrast agent to appearance of minimum of curve.

1H magnetic resonance spectroscopy

1H MRS was performed using 3D CSI PRESS with long echo time (TE = 135 ms). The Voxel matrices were placed in the area of the high signal intensities on the T2W/FLAIR images which corresponded to edema and the contrast enhancement on T1W. The

spectra evaluation was performed using the commercial Syngo v15 workstation (Siemens, Erlangen, Germany), metabolites as choline, chromium, (Cho, Cr), N-acetylaspartate (NAA) and a single peak at 3.56 ppm in long echo time defined as Gly were taken into account. The area under the curve of a metabolite Cho, NAA was considered as relative concentration and was measured in terms of ratios in relation to Cr (Cho/Cr, NAA/Cr).

Statistical analysis

Statistical calculation was performed in the IBM SPSS Statistics17. Comparisons between the obtained mean TTP values between the patient with pseudoprogression and true progression were performed using ANOVA with Bonferroni correction. Statistical significance was set at $p = 0.05$.

Results

In the 3rd week from the beginning of concomitant RT and CMT areas of high signal were observed in FLAIR images both in patients with PSP and RCT. However, no post-contrast enhancement was detected in the T1W images.

In the 10th week from starting the therapy, the MRI examinations demonstrated a new enhancement in the post-contrast T1W images patients, both in patients with PSP and RCT (Figures 1b and 1d). In addition, hyperintensities were observed in the regions of the FLAIR images that correspond to the non-enhancing portion of the lesion in both entities (Figures 1a and 1c). The follow-up MR imaging in the 6th month upon surgery revealed presence of RCT in 32 (80%) patients, while the PSP was established in 8 (20%).

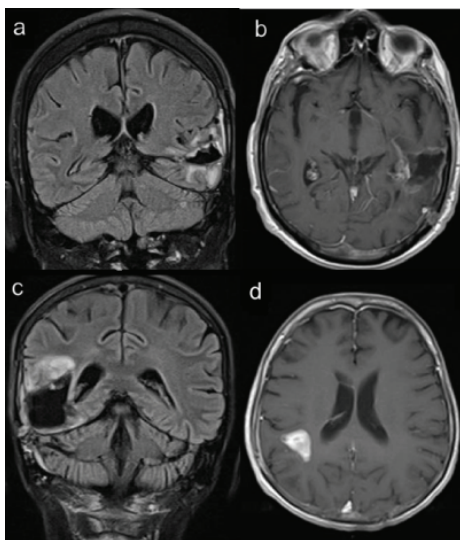


Fig. 1 – FLAIR and post-contrast T1W images obtained in the 10th week after surgery in the patients with true progression (upper row) and pseudoprogression (lower row). Although minute area of post-contrast enhancement was observed in b) and d) pseudoprogression (PSP) and radiation and chemotherapy (RCT). In case of pseudoprogression follow-up, the magnetic resonance imaging (MRI) demonstrated a decrease of region of post-contrast enhancement in both entities [a), c)].

Figure 2 shows the box-whiskers plot of the nCBV values for PSP and RCT in the 3rd and 10th week after surgery. No significant differences were found between the nCBV values in pseudo-progression in the 3rd week (mean 2.94 ± 0.95) and in the 10th week (mean 3.31 ± 1.32) after tumor resection. Also, no significant differences were found between the nCBV values for progressive disease in the 3rd week (mean 2.99 ± 0.97) and in the 10th week (mean 3.30 ± 1.05). Similarly, no differences were found between PSP and RCT when the nCBF values were analyzed (3rd week after surgery: $nCBF(PSP) = 2.62 \pm 1.10$, $nCBF(RCT) = 2.80 \pm 1.41$; 10th week: $nCBF(PSP) = 2.36 \pm 1.24$, $nCBF(RCT) = 2.74 \pm 1.2$).

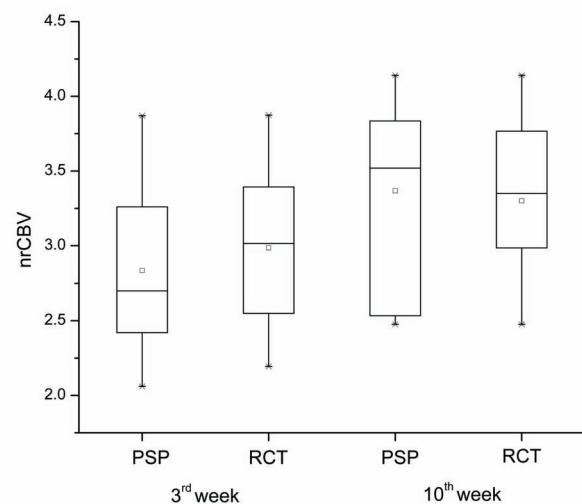


Fig. 2 – Normalized relative cerebral blood volume (arCBV) values for pseudoprogression (PSP) and recurrent tumor (RCT) in the 3rd and 10th week after surgery.

The mean DSC curves for RCT and PSP in the 3rd week and in 10th week after surgery are shown in Figures 3a and 3b.

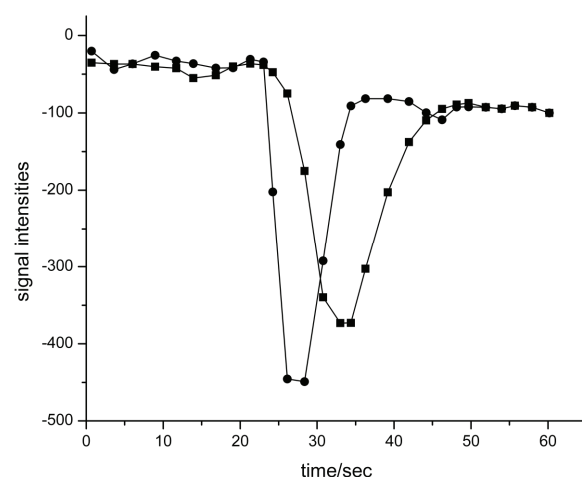


Fig. 3a – Average dynamic susceptibility contrast (DSC) curves in patients with tumor progression in the 3rd week (circles) and the 10th week (squares) after surgery.

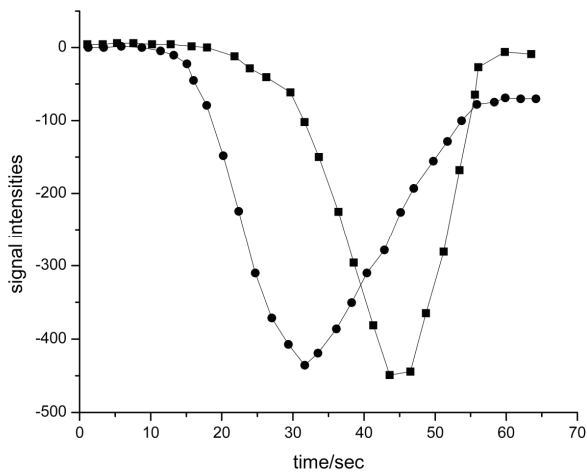


Fig. 3b – Average DSC curves in the patients with pseudoprogression in the 3rd (circles) and the 10th week (squares) after surgery.

Figure 4a shows the box-whiskers plot of TTP values for PSP and RCT in the 10th week after surgical resection. No significant differences ($p > 0.05$) were found between the TTP values in the first (mean 30 ± 5 s) and in the second time point (33 ± 7 s) in the RCT group. A significant difference ($p < 0.05$) was observed when the TTP values for PSP were compared: 32 ± 8 s in the 3rd week and 43 ± 9 s in the 10th week. Also, the TTP values for RCT and PSP differed significantly in the 10th week, but not in the 3rd after surgery.

The receiver operating characteristic (ROC) curves for differentiation RCT from PSP for the 3rd week and the 10th week after surgery are shown in Figures 5a and 5b. It can be noticed that differentiation of PSP and RCT, based on the TTP values observed in the 3rd week after surgery, is characterized by intermediate sensitivity and high specificity (64% and 94% respectively). However, in the 10th week, specific-

ity and sensitivity for their differentiation were 78% and 99% (AUC = 0.86, $p < 0.001$), respectively.

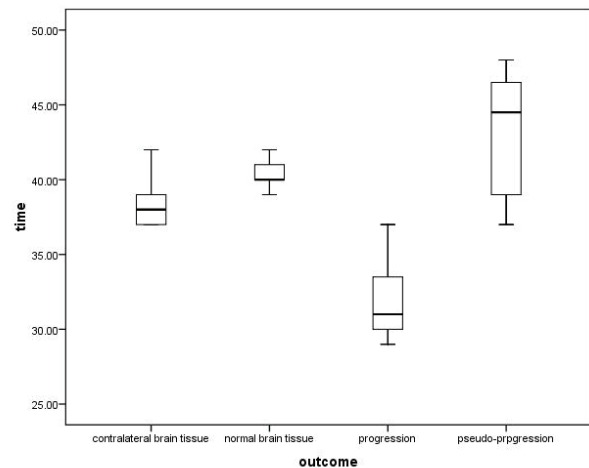


Fig. 4 – The time-to-peak (TTP) values of progression and pseudoprogression in 10th week compared with the TTP values from the normal brain tissue and contralateral brain tissue.

In 1H MR spectra for all 40 patients we observed markedly decreased the NAA/Cr ratios and prominently elevated the Cho/Cr ratio ($\text{Cho/Cr} > 2$) compared to the contralateral normal-appearing brain tissue ($\text{Cho/Cr} = 0.8-1$). The inverted lactate peak could be identified in most of the cases and usually was high in the cystic/necrotic portion of the tumor. Presence of Gly peak at 3.56 ppm was established in spectra of enhancing lesion in 6 (18%) patients with progressive disease (Figure 6b), but not in spectra of pseudoprogression (Figure 6a). The Gly was detected only in solid part of the tumor with the Gly/Cr ratio in range from 0.50 to 0.95. The observed ratio of Gly/Cho was low and range from 0.12 to 0.18.

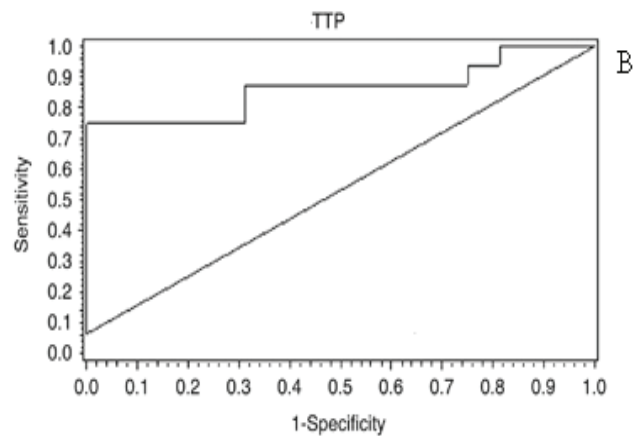
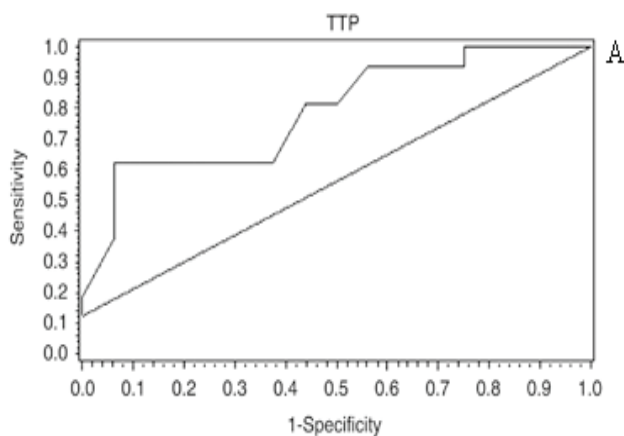


Fig. 5 – Receiver operating characteristic (ROC) curves of perfusion time-to-peak (TTP) for progression and pseudoprogression in A) 3rd and B) 10th week after surgery.

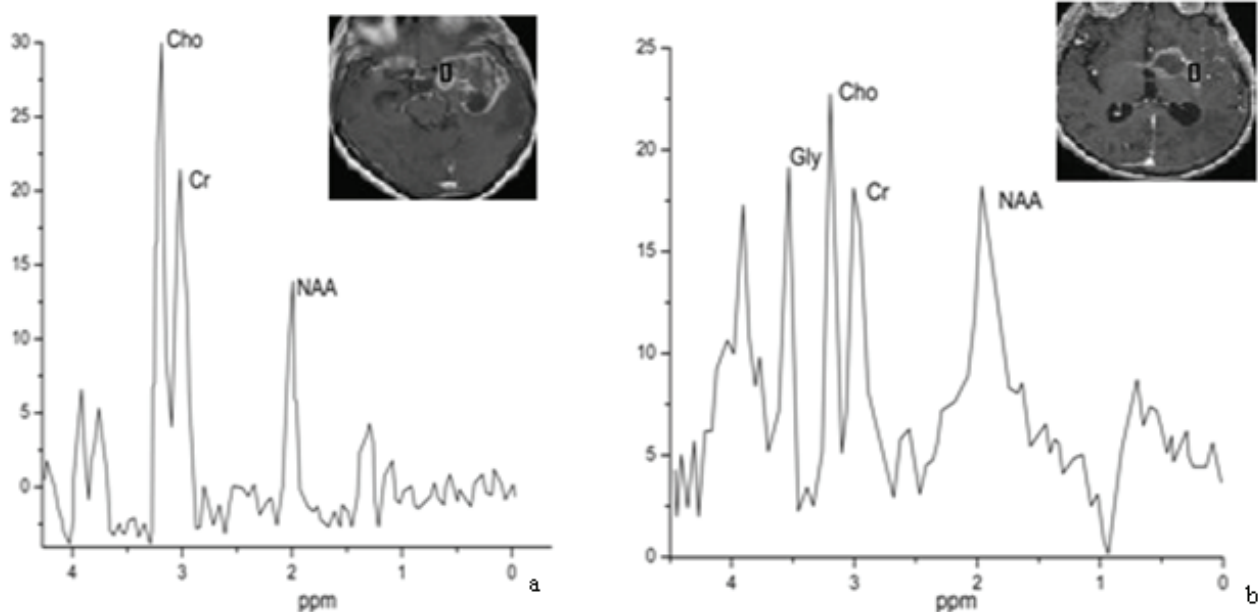


Fig. 6 – ^1H magnetic resonance (MR) spectra with long echo time in the patients with a) pseudo-progression and b) progressive disease in 10th week (glycine peak is present (3.56 ppm) in the spectra of patient with diagnosed progression). The spectroscopic voxel was positioned in the solid part of the tumor.

Discussion

In this study, we used modified (“in-house”) protocol for the MRI assessment of tumor response to combined RT and CMT – the first follow-up MRI was performed in the course of therapy (3rd week after surgery) while the second was performed in the first week after its finalization. The commonly reported protocols employed baseline MRI performed within 48 h after surgery and the second time point is usually within 4–12 weeks after completion of therapy.

We found no significant differences between the nCBV values for PSP and RCT regardless of time point used for comparison. The nCBV values obtained early in the course of therapy (3rd week after surgery) are in agreement with the values previously reported for non-treated GBM, which suggest that no changes in this parameter can be observed at this time point. The finding that nCBV cannot differentiate PSP and RCT in the 10th week after surgery disagrees with the findings of a majority of studies which evaluated the use of nCBV in the assessment of GBM response to therapy^{5, 13, 14}. However, in those studies there were differences in cut-off values and performance of nCBV in differentiation between PSP and RCT. Song et al.¹² and Sugahara et al.²⁷ reported that this parameter had no value in solving this diagnostic dilemma. Leimgruber et al.²⁸ even claimed that nCBV could not distinguish between the RCT and effects of therapy. The absence of concordance between findings of those studies may be attributed to several causes. First, the vasodilatation and inflammation which induced by application of concomitant therapy could lead to overlap in the nCBV values for PSP and RCT. Further, different algorithms for the estimation of perfusion parameters, subjectivity in AIF selection, presence/absence of contrast leakage correction may intro-

duce errors in nCBV determination. For example, using blood pool constrained agent and standard gadolinium based agent, Gahramanov et al.²⁹ demonstrated that absence of correction to leakage of contrast agent may lead to 20% increase in false negative RCTs. Last but not the least, the choice of the ROI positioning may be determining because suspected RCT/PSP may contain portions of tissue that responded to therapy as well as viable tumor¹⁶. Albeit, the procedures involving the advanced analysis of perfusion parameters showed a good performance in distinguishing PSP and RCT^{17–19}, the complexity of their algorithm made them hardly suitable for routine clinical assessment of the GBM response to treatment.

When evaluating the performance of TTP, we found that this parameter, measured in the first week after therapy, could be used in distinguishing RCT and PSP with relatively high specificity and sensitivity. The prolonged TTP in PSP compared to RCT may be explained by presence of inflammation and radiation induced damage of blood vessels and consequent decrease in tissue perfusion. This was partly supported by the lower values (but not significantly) of nCBF in PSP compared with RCT found in this study. In addition, the therapy-induced damage of vessels may result in leakage of contrast agent in interstitium which may lead to an increase in the TTP value. However, the permeability data which would confirm our assumption are available for *de novo*/recurrent GBM and normal tissue, but not for pseudo-progression^{30, 31}. The use of TTP has some advantages over the standard perfusion parameters in the evaluation of GBM response to therapy. The values of rCBV and rCBF highly depend on choice of Arterial Input Function (AIF) which, in turn, relies on an operator’s experience^{21, 32}. Further, local AIF usually does not match that from the large arterial ves-

sels (routinely used for the definition of AIF). In turn, TTP is directly determined from the DSC signal time course and thus does not require any assumptions about AIF which makes the TTP parameter a good choice for unbiased characterization of tissue perfusion²⁰.

We found no significant differences between the Cho/Cr ratios in GBM and pseudoprogression. This is opposite to the reports which claim that Cho/Cr > 2 are characteristic for tumor recurrences³³. However there are studies that compromise ability of this ratio to distinguish pseudoprogression from tumor tissue⁷. It is a well-known fact that neither reduction in the NAA/Cr ratio nor concentrations of NAA are specific in distinguishing brain pathologies³⁴.

Our findings suggest that excess glycine in the region of post-contrast enhancement in treated GBM might pinpoint to rest/reappearance of tumor. To our knowledge, there are no MR spectroscopic studies which dealt with the use of the Gly levels in distinguishing of recurrent tumor from pseudoprogression. However, there are both the biochemical³⁵ and MRI spectroscopic studies^{33,36,37} reporting the increased gly levels of GBM. There are several assumptions about origins of increased levels of this amino acid in high grade tumors. The excess concentration of gly found in GBM may be consequence of altered metabolism of glucose in which 3-phosphoglycerate follows an alternative pathway being converted in 3-phosphoserine and further in serine and gly³⁸. Recently, Chinnayian et al.³⁵ reported altered glucose metabolism in GBM and a severalfold increase in the levels of key metabolites glucose-6-phosphate, ribose-5-phosphate, serine and glycine. This finding could support previous assumption. In turn, the increased levels of inhibitory neurotransmitter glycine may be a response to the excitotoxic levels of glutamate in extracellular space found in the GBM tissue. Although some studies suggest presence of additional gene mutations in RCT compared with primary GBM, there has not been convincing evidence, so far, for differences in their

chemical constitution. This supports our speculation that the increased levels of gly may be indication of presence of RCT.

One of the major limitations of our study is difficulty of precise estimation of Gly which may be hampered by the spectral overlap with the J-coupled resonances of myoinositol (Myo) The J evolution of resonances during the echo time can be exploited for differentiation between the Gly and Myo signals, but it cannot be excluded a contribution from Myo even in long echo times.

Other potential limitation of our study is difficulty in defining pseudoprogression. In our study, we defined pseudoprogression based on the RANO criteria. These criteria were chosen to provide the most potentially useful information to the treating neurooncologist. It is possible that some of the patients who were classified as progressive disease due to a change in treatment, however, could have had pseudoprogression and done well. On the other hand, it is possible that some patients classified as pseudoprogression had slowly progressive tumors, instead.

Our final analysis cohort was relatively small, with a low number of pseudoprogression patients. The magnitude in the differences in the TTP parameter was striking, however a statistical significance was achieved. This suggests that such differences between the two groups are real and robust enough to prompt additional, larger studies.

Conclusion

Non-invasive techniques to detect and quantify the metabolic features and hemodynamic status of human tumor tissue have outstanding clinical potential in cancer imaging. The results implies that changes in Gly levels and TTP may be related to specific signatures that favor better response on therapy and outcome for the GBM patients.

R E F E R E N C E S

1. *Easaw JC, Mason WP, Perry J, Laperriere N, Eisenstat DD, del Maestro R, et al.* Canadian recommendations for the treatment of recurrent or progressive glioblastoma multiforme. *Curr. Oncol* 2011; 18(3): e126–36.
2. *Carlsson SK, Brothers SP, Wablestedt C.* Emerging treatment strategies for glioblastoma multiforme. *EMBO Mol Med* 2014; 6(11): 1359–70.
3. *Macdonald DR, Cascino TL, Schold SC Jr, Cairncross JG.* Response criteria for phase II studies of supratentorial malignant glioma. *J Clin Oncol* 1990; 8(7): 1277–80.
4. *Wen PY, Macdonald DR, Reardon DA, Cloughesy TF, Sorensen GA, Galanis E, et al.* Updated response assessment criteria for high-grade gliomas: Response assessment in neuro-oncology working group. *J Clin Oncol* 2010; 28(11): 1963–72.
5. *Gabramanov S, Raslan AM, Muldoon LL, Hamilton BE, Rooney WD, Varalhyay CG, et al.* Potential for differentiation of pseudoprogression from true tumor progression with dynamic susceptibility-weighted contrast-enhanced magnetic resonance imaging using ferumoxytol vs. gadoteridol: a pilot study. *Int J Radiat Oncol Biol Phys* 2011; 79(2): 514–23.
6. *Morris JG, Grattan-Smith P, Panegyres PK, O'Neill P, Soo YS, Langlands AO.* Delayed cerebral radiation necrosis. *Quarterly J Med* 1994; 87(2): 119–29.
7. *Hygino da Cruz LC Jr, Rodriguez I, Domingues RC, Gasparetto EL, Sorensen AG.* Pseudoprogression and pseudoresponse: imaging challenges in the assessment of posttreatment glioma. *AJNR Am J Neuroradiol* 2011; 32(11): 1978–85.
8. *Chu HH, Choi SH, Ryoo I, Kim SC, Yeom JA, Shin H, et al.* Differentiation of true progression from pseudoprogression in glioblastoma treated with radiation therapy and concomitant temozolomide: comparison study of standard and high-b-value diffusion-weighted imaging. *Radiology* 2013; 269(3): 831–40.
9. *Sub CH, Kim HS, Choi YJ, Kim N, Kim SJ.* Prediction of pseudoprogression in patients with glioblastomas using the initial and final area under the curves ratio derived from dynamic contrast-enhanced T1-weighted perfusion MR imaging. *AJNR Am J Neuroradiol* 2013; 34(12): 2278–86.
10. *Barajas RF Jr, Chang JS, Segal MR, Parsa AT, McDermott MW, Berger MS, et al.* Differentiation of recurrent glioblastoma multiforme from radiation necrosis after external beam radiation therapy with dynamic susceptibility-weighted contrast-

- enhanced perfusion MR imaging. *Radiology* 2009; 253(2): 486–96.
11. Verma N, Comperthwaite MC, Burnett MG, Markey MK. Differentiating tumor recurrence from treatment necrosis: a review of neuro-oncologic imaging strategies. *Neuro Oncol* 2013; 15(5): 515–34.
 12. Song YS, Choi SH, Park CK, Yi KS, Lee WJ, Yun TJ, et al. True progression versus pseudoprogression in the treatment of glioblastomas: a comparison study of normalized cerebral blood volume and apparent diffusion coefficient by histogram analysis. *Korean J Radiol* 2013; 14(4): 662–72.
 13. Kong DS, Kim ST, Kim EH, Lim DH, Kim WS, Sub YL, et al. Diagnostic dilemma of pseudoprogression in the treatment of newly diagnosed glioblastomas: the role of assessing relative cerebral blood flow volume and oxygen-6-methylguanine-DNA methyltransferase promoter methylation status. *AJNR Am J Neuroradiol* 2011; 32(2): 382–7.
 14. Young RJ, Gupta A, Shah AD, Graber JJ, Chan TA, Zhang Z, et al. MRI perfusion in determining pseudoprogression in patients with glioblastoma. *Clin Imaging* 2013; 37(1): 41–9.
 15. Mangla R, Singh G, Ziegelitz D, Milano MT, Korones DN, Zhong J, et al. Changes in relative cerebral blood volume 1 month after radiation-temozolomide therapy can help predict overall survival in patients with glioblastoma. *Radiology* 2010; 256(2): 575–84.
 16. Hu LS, Eschbacher JM, Heiserman JE, Dueck AC, Shapiro WR, Liu S, et al. Reevaluating the imaging definition of tumor progression: Perfusion MRI quantifies recurrent glioblastoma tumor fraction, pseudoprogression, and radiation necrosis to predict survival. *Neuro Oncol* 2012; 14(7): 919–30.
 17. Baek HJ, Kim HS, Kim N, Choi YJ, Kim YJ. Percent change of perfusion skewness and kurtosis: A potential imaging biomarker for early treatment response in patients with newly diagnosed glioblastomas. *Radiology* 2012; 264(3): 834–43.
 18. Cha J, Kim ST, Kim HJ, Kim B, Kim JK, Lee JY, et al. Differentiation of Tumor Progression from Pseudoprogression in Patients with Posttreatment Glioblastoma Using Multiparametric Histogram Analysis. *Am J Neuroradiol* 2014; 35(7): 1309–17.
 19. Tsien C, Galbán CJ, Chenevert TL, Johnson TD, Hamstra DA, Sundgren PC, et al. Parametric response map as an imaging biomarker to distinguish progression from pseudoprogression in high-grade glioma. *J Clin Oncol* 2010; 28(13): 2293–920.
 20. Nasel C, Azizi A, Veintimilla A, Mallek R, Schindler E. A standardized method of generating time-to-peak perfusion maps in dynamic-susceptibility contrast-enhanced MR imaging. *AJNR Am J Neuroradiol* 2000; 21(7): 1195–8.
 21. Neumann-Haefelin T, Wütsack HJ, Wenserski F, Siebler M, Seitz RJ, Mödder U, et al. Diffusion- and perfusion-weighted MRI. The DWI/PWI mismatch region in acute stroke. *Stroke* 1999; 30(8): 1591–7.
 22. Brandes AA, Tosoni A, Spagnoli F, Frezza G, Leonardi M, Calucci F, et al. Disease progression or pseudoprogression after concomitant radiochemotherapy treatment: Pitfalls in neurooncology. *Neuro Oncol* 2008; 10(3): 361–7.
 23. Sundgren PC. MR Spectroscopy in Radiation Injury. *Am J Neuroradiol* 2009; 30(8): 1469–76.
 24. Ye ZC, Sontheimer H. Glioma cells release excitotoxic concentrations of glutamate. *Cancer Res* 1999; 59(17): 4383–91.
 25. Ye ZC, Rothstein JD, Sontheimer H. Compromised glutamate transport in human glioma cells: Reduction-mislocalization of sodium-dependent glutamate transporters and enhanced activity of cystine-glutamate exchange. *J Neurosci* 1999; 19(24): 10767–77.
 26. Righi V, Andronesi OC, Mintzopoulos D, Black PM, Tzika AA. High-resolution magic angle spinning magnetic resonance spectroscopy detects glycine as a biomarker in brain tumors. *Int J Oncol* 2010; 36(2): 301–6.
 27. Sugahara T, Korogi Y, Tomiguchi S, Shigematsu Y, Ikushima I, Kira T, et al. Posttherapeutic intraaxial brain tumor: the value of perfusion-sensitive contrast-enhanced MR imaging for differentiating tumor recurrence from nonneoplastic contrast-enhancing tissue. *AJNR Am J Neuroradiol* 2000; 21(5): 901–9.
 28. Leimgruber A, Ostermann S, Yeon EJ, Buff E, Maeder PP, Stupp R, et al. Perfusion and diffusion MRI of glioblastoma progression in a four-year prospective temozolomide clinical trial. *Int J Radiat Oncol Biol Phys* 2006; 64: 869–75.
 29. Gabrmanov S, Muldoon LL, Varallyay CG, Li X, Kraemer DF, Fu R, et al. Pseudoprogression of glioblastoma after chemo- and radiation therapy: Diagnosis by using dynamic susceptibility-weighted contrast-enhanced perfusion MR imaging with ferumoxytol versus gadoteridol and correlation with survival. *Radiology* 2013; 266(3): 842–52.
 30. Cha S, Yang L, Johnson G, Lai A, Chen MH, Tihan T, et al. Comparison of Microvascular Permeability Measurements, Ktrans, Determined with Conventional Steady-State T1-Weighted and First-Pass T2*-Weighted MR Imaging Methods in Gliomas and Meningiomas. *Am J Neuroradiol* 2006; 27(2): 409–17.
 31. Law M, Yang S, Babb JS, Knopp EA, Golfinos JG, Zagzag D, et al. Comparison of Cerebral Blood Volume and Vascular Permeability from Dynamic Susceptibility Contrast-Enhanced Perfusion MR Imaging with Glioma Grade. *AJNR Am J Neuroradiol* 2004; 25(5): 746–55.
 32. Rempp KA, Brix G, Wenz F, Becker CR, Gückel F, Lorenz WJ. Quantification of regional cerebral blood flow and volume with dynamic susceptibility contrast-enhanced MR imaging. *Radiology* 1994; 193(3): 637–41.
 33. Lehnhardt F, Bock C, Röbn G, Ernestus R, Hoehn M. Metabolic differences between primary and recurrent human brain tumors: A 1H NMR spectroscopic investigation. *NMR Biomed* 2005; 18(6): 371–82.
 34. Ken S, Vieilleveigne L, Franceries X, Simon L, Supper C, Lotterie JA, et al. Integration method of 3D MR spectroscopy into treatment planning system for glioblastoma IMRT dose painting with integrated simultaneous boost. *Radiat Oncol* 2013; 8: 1.
 35. Chinnaiyan P, Kensicki E, Bloom G, Prabhu A, Sarcar B, Kabali S, et al. The metabolomic signature of malignant glioma reflects accelerated anabolic metabolism. *Cancer Res* 2012; 72(22): 5878–88.
 36. Hattingen E, Lanfermann H, Quick J, Franz K, Zanella FE, Pilatus U. 1H MR spectroscopic imaging with short and long echo time to discriminate glycine in glial tumours. *MAGMA* 2009; 22(1): 33–41.
 37. Tugnoli V, Tosi MR, Barbarella G, Bertoluzza A, Ricci R, Trevisan C. In vivo 1H MRS and in vitro multinuclear MR study of human brain tumors. *Anticancer Res* 1996; 16(5A): 2891–9.
 38. Jain M, Nilsson R, Sharma S, Madhusudhan N, Kitami T, Sonza AL, et al. Metabolite profiling identifies a key role for glycine in rapid cancer cell proliferation. *Science* 2012; 336(6084): 1040–4.

Received on January 14, 2017.

Revised on July 4, 2017.

Accepted on July 10, 2017.

Online First September, 2017.